

Side-Information Aided Adaptive Fusion Algorithm for Multiuser Detection in Grant-Free Non-Orthogonal Multiple Access Networks

Han Yuan, Congcong Ma, Kun Yang and Tong Peng*

Abstract—Grant-free non-orthogonal multiple access (GF-NOMA), acting as a promising technique to provide high connection density with low latency, serves multiple users simultaneously with efficient spectrum sharing and simplified resource management. The sparsity of user activity naturally exists in the uplink GF-NOMA system, which makes compressed sensing (CS) technology applied to multi-user detection (MUD). In this paper, we propose a side-information aided adaptive fusion (SIAF) algorithm to improve the MUD performance in the uplink GF-NOMA system. The proposed algorithm reconstructs the signal without knowing the signal sparsity, and makes full use of the structural characteristics of the temporal correlation in the GF-NOMA system to obtain accurate active user estimation. In the post-processing of the algorithm, we obtain low data error rate by fusing two conventional CS algorithms. The simulation results show that our algorithm has better MUD performance than the conventional CS algorithms.

Index Terms—Grant-free non-orthogonal multiple access, compressed sensing, multiuser detection

I. INTRODUCTION

Massive Machine-Type Communications (mMTC) is considered as one of the most important techniques for beyond fifth generation (B5G) wireless networks. It allows the connection of a large number devices and reduction of the need for manual intervention in Internet of Things (IoT) networks [1, 2]. In such networks, non-orthogonal multiple access (NOMA) is widely deployed due to its large-scale connectivity. NOMA works based on the principle of non-orthogonality, which is capable to support multiple devices to send data simultaneously on the same radio resource block by using a user-specific multiple access (MA) signature sequence [3–5]. By using such sequence, the receiver can effectively recover original data and achieve large-scale connection with limited bandwidth and frequencies.

In modern mMTC networks, an IoT device is activated when data is required to be sent, and it goes back to sleep mode when the transmission is done. According to [6], the number of simultaneous active devices takes a small proportion to the total number of devices, even in busy periods. Thus, it is inevitable to apply grant-free techniques in such networks to achieve ultra low latency since most of the devices in current mMTC applications transmit data sporadically. According to

the sparsity nature of user activities in uplink GF-NOMA, it is feasible to resolve the multi-user detection (MUD) problem under the compressed sensing (CS) framework. In [7, 8], CS-based MUD schemes have been proposed. Most of these works are based on standard sparse models. Due to sporadic transmission, their models only consider that the multi-user vectors are sparse, and they do not make full use of the underlying user activity characteristics of the uplink GF-NOMA system. In the uplink GF-NOMA system, the change of active users in several consecutive time slots is slow, that is, there is a common set between the active user set of this time slot and that of the previous time slot. In [9], an algorithm based on dynamic compressed sensing was proposed, the main idea is to use the active user of the previous time slot as the initial active user set. Through this method, the algorithm based on dynamic compressed sensing can obtain a certain bit error rate performance gain. In [10], the author proposes the Modified Orthogonal Matching Pursuit (MOMP) algorithm, which takes the estimated active user set of the previous time slot as the candidate active user set in each iteration of detecting active users. These CS-MUD algorithms[9, 10] use the temporal correlation of the GF-NOMA system, which significantly improves the MUD performance compared to conventional CS algorithms. However, these algorithms require the sparsity of the signal as a prior knowledge, which is not easy to obtain in reality. In [11], the prior-information aided adaptive subspace pursuit (PIA-ASP) algorithm is proposed, the temporal correlation is utilized by introducing the concept of information parameters. However, in some cases, due to the overestimation of the information parameters, the size of the active user set estimated by the PIA-ASP algorithm is larger than the actual user sparsity, and the MUD performance is affected.

In this paper, we propose a side-information aided adaptive fusion (SIAF) algorithm to detect active users in uplink GF-NOMA systems. The main contribution of this paper can be summarized as follows:

- A new adaptive algorithm based on CS is deployed in our design which determines the actual user sparsity iteratively without the prior knowledge of the sparsity of the signal.
- A new refined prior support set selection strategy is proposed in our algorithm, we use the prior support set as the projection base to project the current time slot, retain the index whose energy of the corresponding projection result is larger than the noise threshold.
- A new post-processing stage based on conventional CS

Han Yuan, Congcong Ma, Kun Yang and Tong Peng* are with the School of Information Engineering, Zhejiang Ocean University, and also with Key Laboratory of Oceanographic Big Data Mining and Application of Zhejiang Province, Zhoushan, People's Republic of China (email: yuanhan@zjou.edu.cn, macongcong@zjou.edu.cn, yangkun@zjou.edu.cn, pengtong@zjou.edu.cn). This work was supported by the national natural science foundation of China under grant No. 62341127.

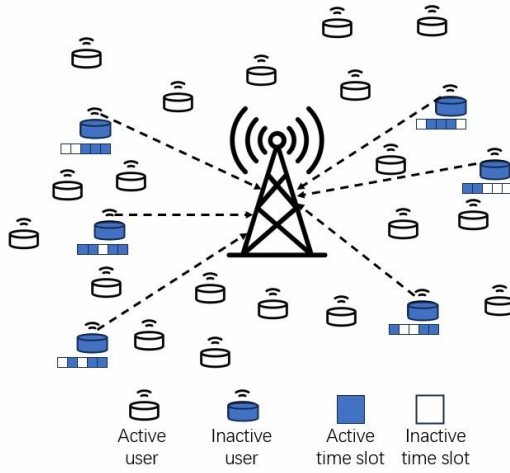


Fig. 1. Illustration of a typical uplink grant-free NOMA system.

algorithms is deployed in our proposed algorithm to shrink the size of potential active user set and achieve higher data detection accuracy.

The rest of this paper is organized as follows. Section II introduces the system model, and Section III presents the details of the proposed algorithm. In Section IV, the computational complexity analysis of the proposed algorithm is provided, following by simulation results in Section V. Section VI concludes the paper.

II. SYSTEM MODEL

In this paper, we consider the uplink scenario of a GF-NOMA system shown in Fig. 1, where K potential users transmitting to BS in a grant free mode. For simplicity and generality, we assume, as in [9–11], that all potential users and base stations are equipped with a single antenna. Given a transmission period, we assume only a small proportion of users are active and most of them stay asleep. After modulation, the transmitted symbol x_k at the k^{th} active user is selected from a complex constellation set χ_0 , e.g., M -QAM. Therefore, the modulated symbols of all users can be denoted by the augmented complex-constellation set $\chi = \chi_0 \cup \{0\}$, where $\{0\}$ denotes the symbols at the inactive users. The transmitted symbol x_k is modulated by a user-specific spread spectrum sequence \mathbf{s}_k with length of N , and then these signals are transmitted simultaneously on the same N orthogonal resources. In order to meet the need of large-scale connection in mMTC, we consider the overload system, i.e., $N < K$.

Since the signals of active users propagate simultaneously through different fading channels, the received signal \mathbf{y} of BS is the superposition of all signals. Therefore, the received signal for the current time slot at BS is given as

$$\begin{aligned} \mathbf{y} &= \sum_{k=1}^K \text{diag}(\mathbf{h}_k) \mathbf{s}_k x_k + \mathbf{w} \\ &= \mathbf{G} \mathbf{x} + \mathbf{w}, \end{aligned} \quad (1)$$

where $\mathbf{h}_k = [h_{1,k}, \dots, h_{N,k}]^T$ denotes the $N \times 1$ coefficient vector of the fading channels, whose elements obey the iden-

tically and independent (i.i.d) complex Gaussian distributions $\mathcal{CN}(0, 1)$, $\text{diag}(\mathbf{h}_k)$ denotes the $N \times N$ diagonal matrix with vector \mathbf{h}_k as the main diagonal element. $\mathbf{s}_k = [s_{1,k}, \dots, s_{N,k}]^T$ is the $N \times 1$ spreading sequence vector of user k , and \mathbf{w} is the noise vector with complex Gaussian distribution $\mathcal{CN}(0, \delta^2 \mathbf{I})$. $\mathbf{x} = [x_1, x_2, \dots, x_K]^T$ is the $K \times 1$ transmitted signal vector for all K users, which is sparse due to the natural sparsity of user activity. \mathbf{G} is the equivalent channel matrix with a dimension of $N \times K$, whose element $g_{n,k}$ in the n^{th} row and the k^{th} column equals to $h_{n,k} \times s_{n,k}$. The main goal at the receiver is to reconstruct the multi-user vector \mathbf{x} from \mathbf{y} to implement joint user activity and data detection when the equivalent channel matrix \mathbf{G} is known. In practical, although the users access or leave the network randomly, some users send information in adjacent time slots. Thus, the objective at the receiver is to reconstruct the transmitted signals $\mathbf{X} = [\mathbf{x}^{[1]}, \mathbf{x}^{[2]}, \dots, \mathbf{x}^{[T]}]$ from the received signals $\mathbf{Y} = [\mathbf{y}^{[1]}, \mathbf{y}^{[2]}, \dots, \mathbf{y}^{[T]}]$, where T denotes successive time slots and $\mathbf{x}^{[t]}$ is the multi-user vector at the t^{th} time slot. In this case, Eq. (1) can be rewrite as

$$\mathbf{y}^{[t]} = \mathbf{G}^{[t]} \mathbf{x}^{[t]} + \mathbf{w}^{[t]}, \quad (2)$$

where $\mathbf{G}^{[t]}$ and $\mathbf{w}^{[t]}$ denote the equivalent channel matrix and the Gaussian noise at the t^{th} time slot, respectively. In this paper, the signal set of the active users at the previous time slot is known as the predictor of the support set at the current time slot, which improves MUD and data detection performances in practical GF-NOMA systems.

III. THE PROPOSED SIDE-INFORMATION AIDED ADAPTIVE FUSION ALGORITHM

Among conventional CS algorithms, the iterative greedy algorithms have received attention due to low complexity and good performance. The most typical greedy algorithms are orthogonal matching pursuit (OMP) [12], subspace pursuit (SP) [13], compressive sampling matching pursuit (CoSaMP) [14]. These conventional CS algorithms need to know the user sparsity as a priori information. In our proposed SIAF algorithm, the actual user sparsity is estimated iteratively. The prior support is used as the projection base to project the current time slot, which can be written as

$$\mathbf{c} = (\mathbf{G}_{\Lambda^{[t-1]}}^{[t]})^\dagger \mathbf{y}^{[t]}, \quad (3)$$

where $\mathbf{G}_{\Lambda^{[t-1]}}^{[t]}$ denotes the $N \times |\Lambda^{[t-1]}|$ submatrix of $\mathbf{G}^{[t]}$ indexed by set $\Lambda^{[t-1]}$, \mathbf{c} is the projection result onto the prior support set, $[\cdot]^\dagger$ represents the Moore-Penrose pseudo-inverse operations of a matrix.

We refine the prior support set by retaining the index whose energy of the corresponding projection result is larger than the noise threshold P_{th} , which can be expressed as

$$\Gamma_p = \{i : \|\mathbf{c}[i]\|_2^2 \geq P_{th}, 1 \leq i \leq K\}. \quad (4)$$

In our proposed algorithm, we calculate the number of elements in the refined prior support set Γ_p as the initial sparsity of the current time slot at the beginning of a new time slot. In addition, Γ_p is also an important part of the active user candidate set in each iteration, which can be written as follows

$$\Gamma^{(i)} = \Gamma_a^{(i)} \cup \Gamma_p \cup S^{[t](i-1)}. \quad (5)$$

In proposed scheme, we can obtain the active user candidate set $\Gamma^{(i)}$ through a greedy method with a fixed sparsity s . When $\|r^{[t](i)}\|_2 < \|r^{[t](i-1)}\|_2$ is triggered, we can obtain s -sparse active user candidate set $\Gamma^{(i)}$, and then we begin to estimate $(s+1)$ -sparse active user candidate set $\Gamma^{(i)}$. Those procedures will be repeated until the $\|r^{[t](i)}\|_2$ reaches the stopping criterion, we get the estimated sparsity s of the signal to be reconstructed and the active user candidate set $\Gamma^{(i)}$.

In this paper, we set the stopping criterion from the perspective of average residual energy. Assume that the sparse signal $\mathbf{x}^{[t]}$ is perfectly reconstructed, the residual $r^{[t](i)}$ of each time slot contains only additive white Gaussian noise. The average energy can have the following constraints

$$\|r^{[t](i)}\|_2^2 \leq \alpha N \delta^2, \quad (6)$$

where $0 < \alpha \leq 1$ denotes the scaling factor. α needs to determine its value according to the specific application scenario, which is given based on experience. According to our experiment, we set the scaling factor $\alpha = 0.8$ after several experiments. Therefore, we set the stopping criterion as $\|r^{[t](i)}\|_2^2 \leq \epsilon$ with $\epsilon = \alpha N \delta^2$, where δ^2 is related to noise, and N is the length of the signal received at the BS.

In the post-processing method of the algorithm, we fuse the classical two algorithms SP algorithm and OMP algorithm. Both algorithms select the active user set from the active user candidate set $\Gamma^{(i)}$. In order to ensure the accuracy of active user estimation and make the number of elements in the estimated active user set as close as possible to the actual user sparsity, we further expand the size of the active user set obtained by the two algorithms on the basis of the estimated sparsity s , which can be expressed as

$$b = \beta * s. \quad (7)$$

β is a new scaling factor, which needs to determine its value according to the noise of the application scenario. We select b users with the largest energy from the active user candidate set $\Gamma^{(i)}$ to get set Λ_a , which can be written as

$$\Lambda_a = \arg \max_b \left\| \left[(G_{\Gamma^{(i)}}^{[t]})^\dagger y^{[t]} \right] \right\|_2. \quad (8)$$

Then we estimate the active user set Λ_b from the set $\Gamma^{(i)}$ according to the main idea of the OMP algorithm. In order to improve the accuracy of the estimated active users, we take the intersection of the two sets to get $\Lambda^{[t]}$, which can be expressed as

$$\Lambda^{[t]} = \Lambda_a \cap \Lambda_b. \quad (9)$$

If the size of $\Lambda^{[t]}$ is less than the sparsity s , we first remove the elements in the set $\Lambda^{[t]}$ from the set $\Gamma^{(i)}$ to obtain the set Λ_c . Next, we add each element in Λ_c to the set $\Lambda^{[t]}$ in turn to get the set Λ_d . Then calculate the residual in each case, which can be written as

$$\mathbf{R}_n(\mathbf{g}) = \mathbf{y}^{[t]} - \mathbf{G}_{\Lambda_d}^{[t]} (\mathbf{G}_{\Lambda_d}^{[t]})^\dagger \mathbf{y}^{[t]} \quad (10)$$

After that we compare the residual energy corresponding to these elements in Λ_c , and retain the element with the smallest

residual energy in $\Lambda^{[t]}$. Repeat this process until the number of elements in the active user set $\Lambda^{[t]}$ reaches the estimated sparsity s . In this way, we get the estimated active user set $\Lambda^{[t]}$ of our algorithm. Next, we get the estimated sparse solution $\hat{\mathbf{x}}^{[t]}$ according to least squares. After that, we begin to find the sparse solution for next time slot.

IV. COMPUTATIONAL COMPLEXITY ANALYSIS

In this section, we analyze the computational complexity of the proposed algorithm. For simplicity, we assume that the system serves K potential users with N resources, the sparsity in each iteration is s . Thus, the computational complexity of the SIAF algorithm in each iteration can be approximately calculated as

- Support estimation: Since the size of matrix $G^{[t]}$ is $N \times K$, the complexity is $O(NK)$.
- LS estimation: It has the complexity on the order of $O(s'^3 + Ns')$, where $s' = \|\Gamma^{(i)}\|_0$ in each iteration.
- Residue update: The complexity of computing the residual is $O(s^3 + 2Ns)$.
- Post-processing : The complexity is $O(s'^3 + Ns' + bs'N + \sum_{i=1}^b (i^3 + 2Ni) + n(s' - \|\Lambda^{[t]}\|_0)(s^3 + 2Ns))$, where n is related to the estimated sparsity s and the intersection of Λ_a and Λ_b .

Besides, the complexity of obtaining the refined prior support set Γ_p before each time slot starts to iterate is $O(\|\Lambda^{[t-1]}\|_0^3 + \|\Lambda^{[t-1]}\|_0 N)$. At the end of each time slot, the complexity of the estimated signal is $O(\|\Lambda^{[t]}\|_0^3 + \|\Lambda^{[t]}\|_0 N)$.

V. SIMULATION RESULT

In this section, we evaluate the proposed SIAF algorithm in the uplink GF-NOMA system in terms of data recovery accuracy performance. Conventional CS-based algorithms, such as OMP [12], OLS and SP[13] algorithms, are used as benchmarks. The number of potential users is $K = 200$, and the length of the spreading sequence is $N = 100$. The spreading matrix is designed as a Gaussian matrix whose components are realized from i.i.d. Gaussian sources $\mathcal{N}(0, 1)$. The number of the continuous time slots is set to $T = 8$. Quadrature Phase Shift Keying (QPSK) is employed for simplicity. The P_{th} and β used in the proposed algorithm is respectively set as 0.56, 0.50, 0.46, 0.36, 0.34, 0.30, and 1.34, 1.20, 1.10, 1.10, 1.10, at the SNR of 0dB, 2dB, 4dB, 6dB, 8dB, 10dB which are selected experimentally.

Fig. 2 shows the symbol error rate (SER) performance comparison of the considered algorithms. The active user set in each time slot set between 18 and 20, i.e., $\|\Lambda^{(t)}\|_0 \sim U(18, 20)$. The size of common portion of the active user set in adjacent time slots also varies from 16 to 18, i.e., $\|\Lambda^{(t)} \cap \Lambda^{(t-1)}\|_0 \sim U(16, 18)$. We set the quality parameter in the PIA-ASP[11] algorithm to 16. From Fig. 2, it can be observed that the SER performance of the proposed algorithm is significantly better than the conventional CS-based algorithms (OMP and SP) and MOMP[10] over the whole range of SNRs. The reason why the SER performance of our algorithm is better than that of the MOMP algorithm is that the

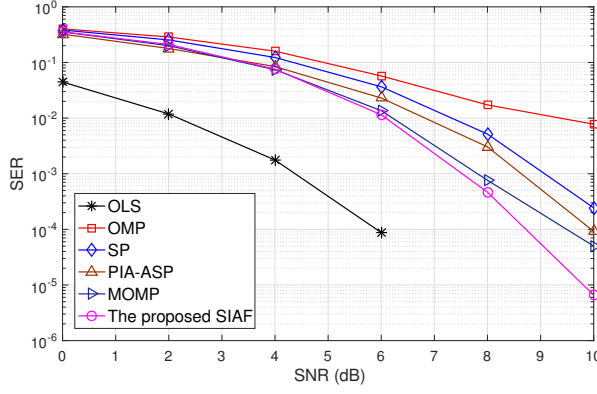


Fig. 2. The SER performance comparison of the considered algorithms with $\|\Lambda^{(t)}\|_0 \sim U(18, 20)$ and $\|\Lambda^{(t)} \cap \Lambda^{(t-1)}\|_0 \sim U(16, 18)$.

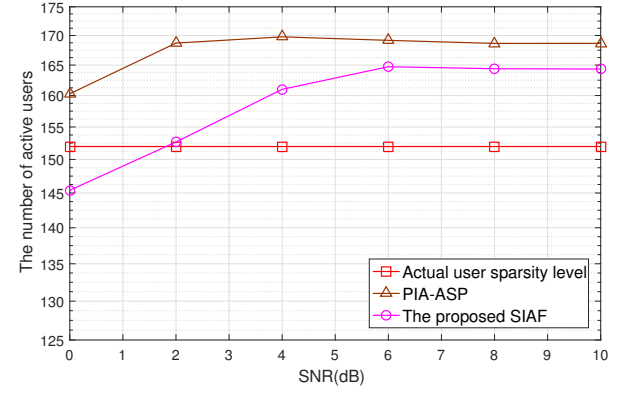


Fig. 4. The number of active users detected by considered algorithms with $\|\Lambda^{(t)}\|_0 \sim U(18, 20)$ and $\|\Lambda^{(t)} \cap \Lambda^{(t-1)}\|_0 \sim U(10, 16)$.

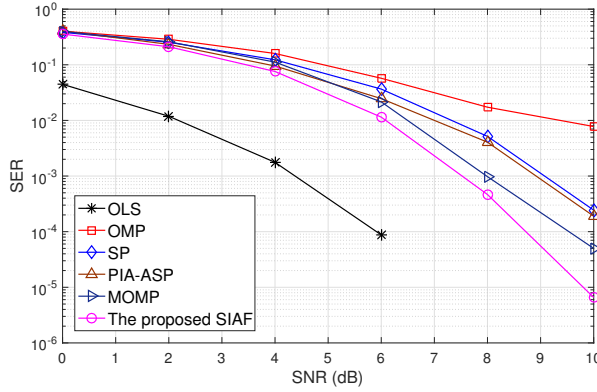


Fig. 3. The SER performance comparison of the considered algorithms with $\|\Lambda^{(t)}\|_0 \sim U(18, 20)$ and $\|\Lambda^{(t)} \cap \Lambda^{(t-1)}\|_0 \sim U(10, 16)$.

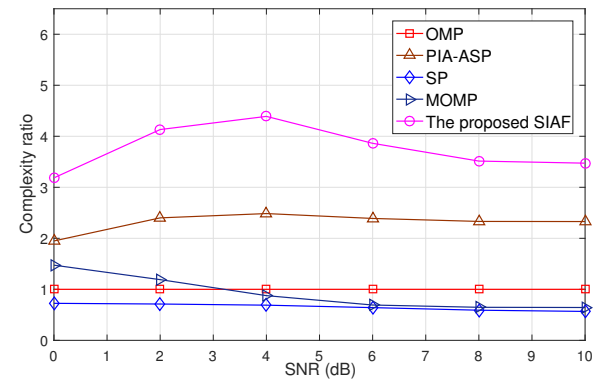


Fig. 5. Complexity ratio comparison of the considered algorithms with $\|\Lambda^{(t)}\|_0 \sim U(18, 20)$ and $\|\Lambda^{(t)} \cap \Lambda^{(t-1)}\|_0 \sim U(10, 16)$.

prior support set used in our algorithm is refined. When SNR is 0.2, the SER performance of our algorithm is worse than that of PIA-ASP algorithm. Because the information parameter in PIA-ASP algorithm is lower than the number of common set of active users in adjacent time slots. Compared with our algorithm, the PIA-ASP algorithm has an important prior knowledge that the set of common active users in adjacent time slots does not exceed information parameter, which causes the SER performance of our algorithm to be worse than that of the PIA-ASP algorithm when SNR is small. When the SNR gradually increases, the SER performance of our algorithm is improved by nearly 1.5dB compared with the PIA-ASP algorithm.

In Fig. 3, the change of the number of active users in each time slot is the same as above, and the number of active the size of common portion of the active user set in adjacent time slots also varies from 10 to 16, i.e., $\|\Lambda^{(t)} \cap \Lambda^{(t-1)}\|_0 \sim U(10, 16)$. In this case, the information parameter in the PIA-ASP algorithm is set to 14, and information parameter will be overestimated in some time slots. In Fig. 3, it is clear that the proposed algorithm significantly outperforms PIA-ASP algorithm, OMP algorithm, SP algorithm and MOMP algorithm for all SNRs. The OLS algorithm outperforms the other algorithms, since it knows the actual active user set.

In Fig. 4, the sum of the number of active users detected by our algorithm and the PIA-ASP algorithm in 8 consecutive time slots is compared with the same simulation conditions in Fig. 3. Both two algorithms reconstruct the sparse signal without the sparsity of the signal to be reconstructed, so the number of active users detected by these two algorithms has a certain error compared with the actual user sparsity. The number of active users detected by our algorithm is closer to the actual user sparsity than the active users detected by the PIA-ASP algorithm.

In Fig. 5, the computational complexity of the considered algorithms is compared with the same simulation conditions in Fig. 3. In order to achieve fair conditions, OMP is treated as a comparative benchmark. The computational complexity ratio is the ratio of the complexity of the considered algorithm to the complexity of the OMP algorithm. We observe that the computational complexity of the PIA-ASP algorithm and our proposed algorithm is higher than other algorithms. The reason is that the signal sparsity is adaptively obtained in these two algorithms, which will generate additional overhead and require additional complexity. The computational complexity of our proposed algorithm is higher than that of PIA-ASP algorithm, because our algorithm fuses two conventional algorithms in the post-processing stage, which will bring additional complexity.

The impact of additional complexity can be mitigated by distributed computing and edge computing at BS.

VI. CONCLUSIONS

In this paper, we study the problem of MUD for uplink GF-NOMA system deploying CS-based techniques, and propose a new side-information aided adaptive fusion algorithm to enhance the MUD and data recovery accuracy. In the proposed algorithm, the sparsity of signal to be reconstructed is not required to be used as an essential prior information. In the algorithm we start from the initial sparsity and gradually estimates the signal sparsity through iteration. In addition, in the algorithm we fuse two CS algorithms in post-processing to improve SER performance. Simulation results have shown that the proposed algorithm can achieve better SER performance over the conventional CS-based MUD algorithms in GF-NOMA system.

REFERENCES

- [1] C. Bockelmann *et al.*, "Towards massive connectivity support for scalable mMTC communications in 5G networks," *IEEE Access*, vol. 6, pp. 28969–28992, 2018.
- [2] Y. Wang and Z. Tian, "Big data in 5G," in *Encyclopedia of Wireless Networks*. Springer, Mar. 2018.
- [3] N. Ye, H. Han, L. Zhao, and A.-H. Wang, "Uplink nonorthogonal multiple access technologies toward 5G: A survey," *Wireless Commun. Mobile Comput.*, vol. 2018, pp. 1–26, Jun. 2018.
- [4] M. Vaezi, G. A. Aruma Baduge, Y. Liu, A. Arafa, F. Fang, and Z. Ding, "Interplay between NOMA and other emerging technologies: A survey," *IEEE Trans. Cogn. Commun. Netw.*, vol. 5, no. 4, pp. 900–919, Dec. 2019.
- [5] L. Dai, B. Wang, Z. Ding, Z. Wang, S. Chen, and L. Hanzo, "A survey of non-orthogonal multiple access for 5G," *IEEE Commun. Surveys Tuts.*, vol. 20, no. 3, pp. 2294–2323, 3rd Quart., 2018.
- [6] J. P. Hong, W. Choi, and B. D. Rao, "Sparsity controlled random multiple access with compressed sensing," *IEEE Trans. Wireless Commun.*, vol. 14, no. 2, pp. 998–1010, Feb. 2015.
- [7] Y. Du, C. Cheng, B. Dong, Z. Chen, X. Wang, J. Fang, and S. Li, "Block-sparsity-based multiuser detection for uplink grant-free NOMA," *IEEE Trans. Wireless Commun.*, vol. 17, no. 12, pp. 7894–7909, Dec. 2018.
- [8] B. Shim and B. Song, "Multiuser detection via compressive sensing," *IEEE Commun. Lett.*, vol. 16, no. 7, pp. 972–974, Jul. 2012.
- [9] B. Wang, L. Dai, Y. Zhang, T. Mir, and J. Li, "Dynamic compressive sensing-based multi-user detection for uplink Grant-free NOMA," *IEEE Commun. Lett.*, vol. 20, no. 11, pp. 2320–2323, Nov. 2016.
- [10] O. O. Oyerinde, "Modified Orthogonal Matching Pursuit (MOMP)-based Multiuser Detector for Uplink NOMA Systems," in *2019, 13th International Conference on Signal Processing and Communication Systems (ICSPCS)*, Gold Coast, QLD, Australia, 2019, pp. 1–5.
- [11] Y. Du, B. Dong, Z. Chen, X. Wang, Z. Liu, P. Gao and S. Li, "Efficient multi-user detection for uplink grant-free NOMA: Prior-information aided adaptive compressive sensing perspective," *IEEE J. Sel. Areas Commun.*, vol. 35, no. 12, pp. 2812–2828, Dec. 2017.
- [12] J. A. Tropp and A. C. Gilbert, "Signal recovery from random measurements via orthogonal matching pursuit," *IEEE Trans. Inf. Theory*, vol. 53, no. 12, pp. 4655–4666, Dec. 2007.
- [13] W. Dai and O. Milenkovic, "Subspace pursuit for compressive sensing signal reconstruction," *IEEE Trans. Inf. Theory*, vol. 55, no. 5, pp. 2230–2249, May. 2009.
- [14] D. Needell and A. Tropp, "CoSaMP: Iterative signal recovery from incomplete and inaccurate samples," *Appl. Comput. Harmon. Anal.*, vol. 26, no. 3, pp. 301–321, Jul. 2009.

Algorithm 1 The Proposed SIAF Algorithm

Input:
 Received signals : $\mathbf{Y} = [\mathbf{y}^{[1]}, \mathbf{y}^{[2]}, \dots, \mathbf{y}^{[T]}]$;
 Equivalent Channel Matrices : $\mathbf{G}^{[1]}, \mathbf{G}^{[2]}, \dots, \mathbf{G}^{[T]}$;

Output:
 Reconstructed sparse signal $\hat{\mathbf{X}} = [\hat{\mathbf{x}}^{[1]}, \hat{\mathbf{x}}^{[2]}, \dots, \hat{\mathbf{x}}^{[T]}]$;

- 1: the initial time slot index $t = 1$ and the prior support set $\Gamma_p = \emptyset$;
- 2: **for** $t = 1$ to T **do**
- 3: **if** $t = 1$ **then**
- 4: $\mathbf{s} = \mathbf{0}$;
- 5: **else**
- 6: $\mathbf{c} = (\mathbf{G}_{\Lambda_{[t-1]}}^{[t]})^\dagger \mathbf{y}^{[t]}$;
- 7: $\Gamma_p = \{\mathbf{i} : \|\mathbf{c}[\mathbf{i}]\|_2^2 \geq \mathbf{P}_{th}, 1 \leq \mathbf{i} \leq \mathbf{K}\}$;
- 8: $\mathbf{s} = \|\Gamma_p\|_0$;
- 9: **end if**
- 10: the iterative index $i = 1$, the support set $\mathbf{S}^{[t](i-1)} = \emptyset$, the residual vector $\mathbf{r}^{[t](i-1)} = \mathbf{y}^{[t]} - \mathbf{G}_{\Gamma_p}^{[t]} (\mathbf{G}_{\Gamma_p}^{[t]})^\dagger \mathbf{y}^{[t]}$;
- 11: **while** $\|\mathbf{r}^{[t](i)}\|_2^2 \geq \epsilon$ **do**
- 12: $\Gamma_a^{(i)} = \arg \max_{\mathbf{s}} \left\| [(\mathbf{G}^{[t]})^\dagger \mathbf{H}_{\mathbf{r}^{[t](i-1)}}] \right\|_2$;
- 13: $\Gamma^{(i)} = \Gamma_a^{(i)} \cup \Gamma_p \cup \mathbf{S}^{[t](i-1)}$;
- 14: $\mathbf{E}_{\Gamma^{(i)}} = (\mathbf{G}_{\Gamma^{(i)}}^{[t]})^\dagger \mathbf{y}^{[t]}, \mathbf{E}_{\{1 \dots \mathbf{K}\} \setminus \Gamma^{(i)}} = \mathbf{0}$;
- 15: $\hat{\mathbf{S}}^{[t](i)} = \arg \max_{\mathbf{s}} \|\mathbf{E}\|_2$;
- 16: $\mathbf{r}^{[t](i)} = \mathbf{y}^{[t]} - \mathbf{G}_{\hat{\mathbf{S}}^{[t](i)}}^{[t]} (\mathbf{G}_{\hat{\mathbf{S}}^{[t](i)}}^{[t]})^\dagger \mathbf{y}^{[t]}$;
- 17: **if** $\|\mathbf{r}^{[t](i)}\|_2 < \|\mathbf{r}^{[t](i-1)}\|_2$ **then**
- 18: $\mathbf{S}^{[t](i)} = \hat{\mathbf{S}}^{[t](i)}, \mathbf{i} = \mathbf{i} + 1$;
- 19: **else**
- 20: $\mathbf{S}^{[t](i)} = \hat{\mathbf{S}}^{[t](i-1)}, \mathbf{s} = \mathbf{s} + 1$;
- 21: **end if**
- 22: **end while**
- 23: $\mathbf{b} = \beta * \mathbf{s}$;
- 24: $\Lambda_a = \arg \max_{\mathbf{b}} \left\| [(\mathbf{G}_{\Gamma^{(i)}}^{[t]})^\dagger \mathbf{y}^{[t]}] \right\|_2$;
- 25: $\mathbf{R} = \mathbf{y}^{[t]}$;
- 26: **for** $j = 1$ to \mathbf{b} **do**
- 27: $\mathbf{q} = \arg \max_{\mathbf{q}} \left\| [(\mathbf{G}_{\Gamma^{(i)}}^{[t]})^\dagger \mathbf{H}_{\mathbf{R}}] \right\|_2$;
- 28: $\Lambda_b = \Lambda_b \cup \{\mathbf{q}\}$;
- 29: $\mathbf{R} = \mathbf{y}^{[t]} - \mathbf{G}_{\Lambda_b}^{[t]} (\mathbf{G}_{\Lambda_b}^{[t]})^\dagger \mathbf{y}^{[t]}$;
- 30: **end for**
- 31: $\Lambda^{[t]} = \Lambda_a \cap \Lambda_b$;
- 32: **if** $\|\Lambda^{[t]}\|_0 < \mathbf{s}$ **then**
- 33: **for** $f = 1$ to $\mathbf{s} - \|\Lambda^{[t]}\|_0$ **do**
- 34: $\Lambda_c = \Gamma^{(i)} \setminus \Lambda^{[t]}$;
- 35: **for** $g = 1$ to $\|\Lambda_c\|_0$ **do**
- 36: $\Lambda_d = \Lambda^{[t]} \cup \Lambda_c(g)$;
- 37: $\mathbf{R}_n(g) = \mathbf{y}^{[t]} - \mathbf{G}_{\Lambda_d}^{[t]} (\mathbf{G}_{\Lambda_d}^{[t]})^\dagger \mathbf{y}^{[t]}$;
- 38: **end for**
- 39: $\mathbf{p} = \arg \min \|\mathbf{R}_n\|_2$;
- 40: $\Lambda^{[t]} = \Lambda^{[t]} \cup \{\mathbf{p}\}$;
- 41: **end for**
- 42: **end if**
- 43: $\hat{\mathbf{x}}_{\Lambda^{[t]}}^{[t]} = (\mathbf{G}_{\Lambda^{[t]}}^{[t]})^\dagger \mathbf{y}^{[t]}, \hat{\mathbf{x}}_{\{1 \dots \mathbf{K}\} \setminus \Lambda^{[t]}}^{[t]} = \mathbf{0}$;
- 44: **end for**
